M. Revilla-León, M. J. Meyer, M. Özcan

Metal additive manufacturing technologies: literature review of current status and prosthodontic applications

Abstract

Objectives: To review the current metal-based additive manufacturing (AM) technologies, namely powder bed fusion (PBF) technologies, and their current prosthodontic applications. The PBF technologies reviewed are selective laser sintering (SLS), selective laser melting (SLM), and electron beam melting (EBM).

Materials and methods: The literature on metal AM technologies was considered, and the AM procedures and their current applications in prosthodontics were collated and described. Published articles about AM metal in dental care were searched (MEDLINE, EMBASE, EBSCO, and Web of Science). All studies related to the description, analysis, and evaluation of prosthodontic applications using metal AM technologies.

Results and conclusions: AM technologies are reliable for many applications in dentistry, including metal frameworks for removable partial dentures (RPDs), overdentures, tooth- and implant-supported fixed dental prostheses (FDPs), and metal frameworks for splinting implant impression abutments. However, further studies are needed in future to evaluate the accuracy, reproducibility, and clinical outcome throughout function of AM technologies.

Keywords: *3D printing, additive manufacturing technologies, electron beam melting, metal, selective laser melting, selective laser sintering, prosthodontics*

Introduction

Conventional casting and subtractive computer-aided manufacturing (CAM) technologies are the most common methods used by dentists to manufacture dental prosthetics.[1] CAM technologies typically refer to a computer numerically controlled (CNC) system, which controls power-driven machine tools. Under the direction of computer software, these tools mechanically remove material from a block form to achieve the desired framework.[2-4] Although these technologies are considered the gold standard for the fabrication of fixed dental prostheses (FDPs), subtractive technologies present a number of manufacturing limitations. These limitations include a considerable amount of wasted raw material (unused remnants of the milling block), the short running cycle of the milling tool due to the abrasive wear of milling, and the space limitations imposed by the size of the milling burs and the axis of the CNC machine, which in turn limit access to smaller areas of the milling block.[5-7]

Additive manufacturing (AM) procedures, in which a powder or liquid base material is built into a solid object, provide a promising alternative manufacturing method.[8,9] The American Society for Testing and Materials (ASTM International) has defined AM technology as "a process of joining materials to make objects from 3D model data, usually layer upon layer, as opposed to subtractive manufacturing (SM) methodologies."[10] The industry standard computer-aided design (CAD) data file format is Standard Triangulation Language (STL), in which boundaries are represented by triangular facets.[11]

In 2008, the ASTM International Technical Committee F42 on AM technologies outlined seven AM categories: stereolithography (SLA), material jetting, material extrusion, binder jetting, powder bed fusion (PBF), sheet lamination, and direct energy deposition.[10] PBF technologies are most commonly used for 3D metal printing in dentistry. There are three types of PBF technologies: selective laser sintering (SLS), selective laser melting (SLM), and electron beam melting (EBM).[10]

Selective laser sintering (SLS)

In 1989, Carl Deckard, along with Joe Beaman, developed and patented SLS technology.[12,13] During this procedure, a high-powered laser (Nd:YAG laser) beam is focused onto a bed of powdered metal, which then fuses into a thin solid layer (20 to100 µm). Another layer of powder is then laid down, which becomes the next slice of the framework. The laser then fuses the top layer with the layer beneath. This process is repeated until the three-dimensional (3D) object is built (Fig 1).[14]

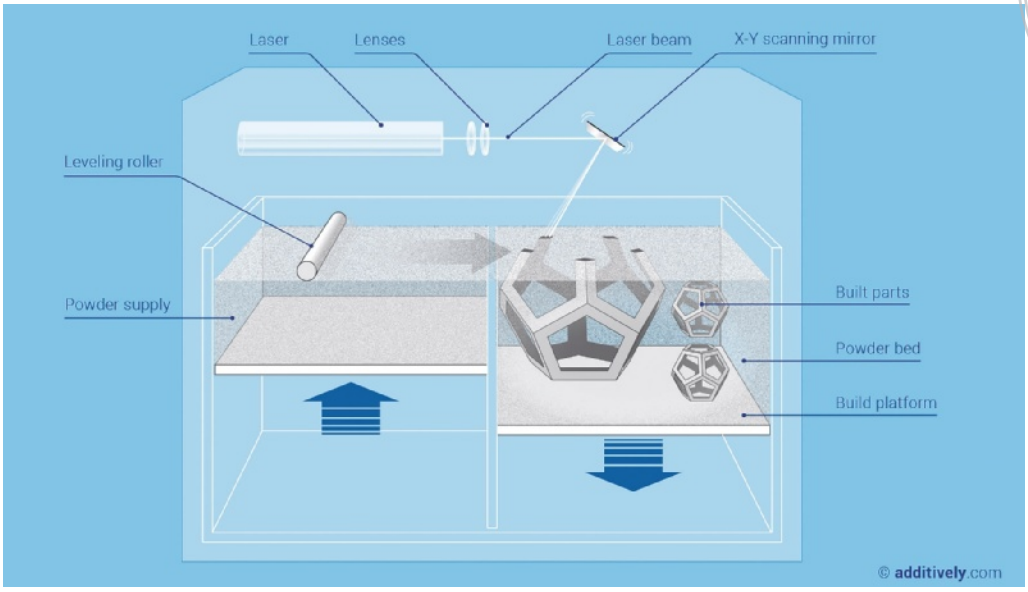

Fig 1 Selective laser sintering (SLS) AM technology scheme. Illustration courtesy of additively.com.

The fabrication chamber is sealed and maintained at a temperature just below the melting point at which the metal powder sinters. This partial melting phenomenon was modeled in 2002 by Fisher et al.[15] Objects made by partial melting are characterized by high porosity, with initially only point contacts between the particles. During laser heating, various sintering and rearrangement mechanisms induce powder binding and densification. Using the partial melting sintering methodology, complete elimination of the porosity is generally not possible, as repulsive forces arise between particles at a high fraction of the liquid binding component.[16]

Selective laser melting (SLM)

Due to the development of powerful high-quality lasers, the partial melting of SLS has been replaced by complete melting; these newer technologies are referred to as metal laser sintering (MLS) or selective laser melting (SLM) technologies.[17-20] Although the superficial finish is highly regarded, thermal gradients induced during the manufacturing process cause high internal stress in the finished component and therefore require post-build heat treatment.[19] The most common fiber laser used for processing metal powders in SLM technology is the CO_2 laser (1 to 2 kW).[20] The building plate can be preheated up to 200°C (Fig 2).[20]

Electron beam melting (EBM)

Instead of using a laser beam (60 kW) to melt or sinter powder, EBM technologies use a focused electron beam to selectively and fully melt layers of powder (100 µm) in an inert environment such as purified argon. During this process, an elevated temperature of about 700°C is maintained in the chamber to reduce residual stresses. First, a tungsten lament is heated above 3000°C, which causes electrons to be emitted. Then, a potential difference between a cathode and an anode causes the electrons to accelerate. The electrons are focused and detected using magnetic coils to form a narrow, high-energy beam that strikes the surface of the powder. When this happens, the kinetic energy transferred through friction creates the necessary heat to melt the metal powder (Fig 3).[18,21]

Many process variables are specific for PBF devices.[22] The main differences between the various PBF technologies are operational parameters such as melting temperature, energy source, energy power, laser beam absorption/reflection coefficients, thermal conductivity, chamber conditions, and temperature reached; other parameters include layer thickness, build orientation, and grain size.[22-24]

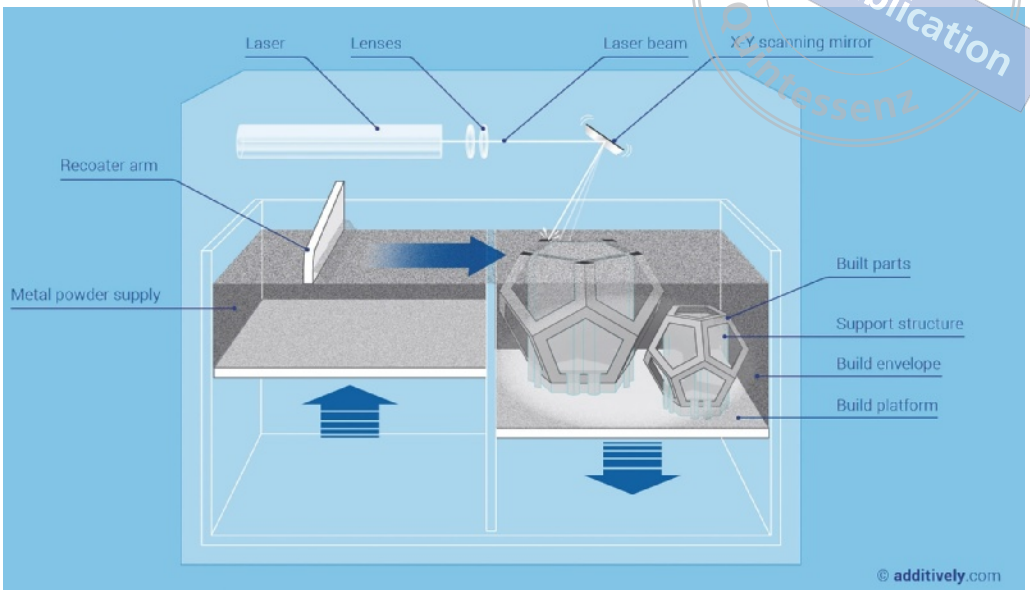

Fig 2 Selective laser melting (SLM) AM technology scheme. Illustration courtesy of additively.com.

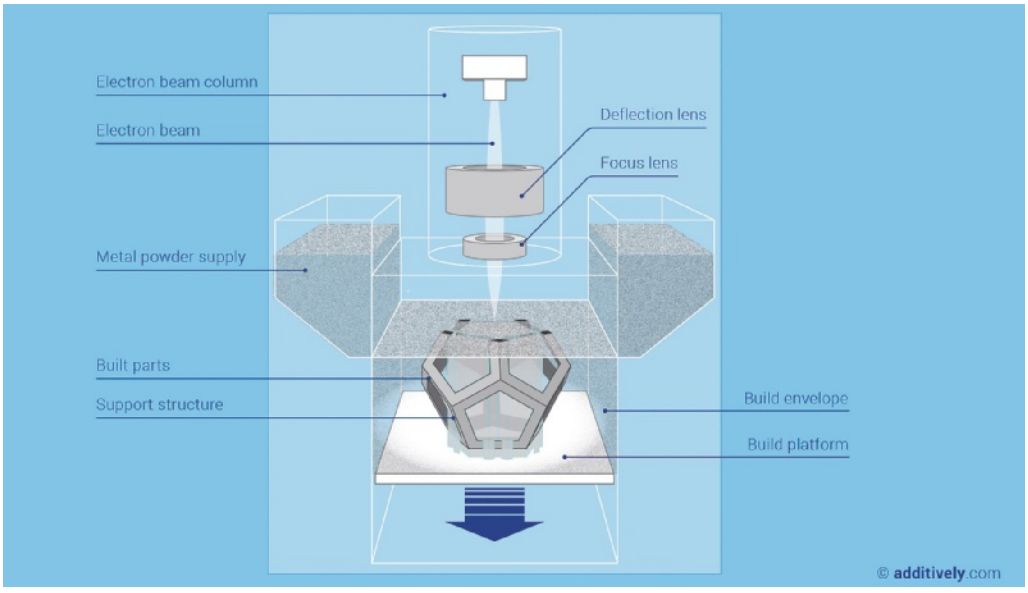

Fig 3 Electron beam melting (EBM) AM technology scheme. Illustration courtesy of additively.com.

Metals used in dentistry for AM

In general, the two primary metals titanium (Ti) and cobalt-chromium (CoCr) are viable for 3D metal printing in dentistry. CoCr powder is primarily composed of cobalt and chromium, but molybdenum, tungsten, silicon, cerium, iron, manganese, and carbon are also present. The powder, which is free of nickel and beryllium, consists of particles between 3 and 14 µm in size.[22-25] However, each system uses different CoCr metal powders (Tables 1 and 2).[22] The most common alloy used in technical, medical, and dental applications is Ti (Ti_6Al_4V).[26-29] As with the CoCr alloys for AM technologies, the Ti powder composition varies between the different technologies (Tables 3 and 4).

Table 1 Chemical composition of CoCr alloys provided by their manufacturers

Brand name	Composition (% wt)	
EOS CoCr MP1	Co: 60–65 Cr: 26–30 Mo: 5–7 Si < 1	Fe < 0.75 Mn < 1 C < 0.16 Ni < 0.1
EOS CoCr SP2	Co: 63.8 Cr: 24.7 Mo: 5.1 W: 5.4 Si: 1	Fe < 0.5 Mn < 0.1
SLM Solutions	Not provided	
3D Systems LayerWise CoCr ASTM F75	Co: Balance Cr: 27–30 Mo: 5–7 W < 0.2 Si < 1	Fe < 0.75 Mn < 1 C < 0.35 Ni < 0.5 B,S < 0.01 P < 0.02 Al, Ti < 0.1 N < 0.25
3D Systems LayerWise CoCr 3DS Dentwise	Co: 59 Cr: 25 W: 9.5 Mo: 3.5 Si: 1	C, Fe, Mn, N < 1.5
Concept Laser	Co: 63.8 Cr: 24.7 Mo: 5.1 W: 5.4 Si: 1	Fe < 0.5 Mn < 0.1
BEGO	Co: 63.9 Cr: 24.7 W: 5.4 Mo: 5.0 Si < 1	

Mechanical properties

The recommended mechanical properties for the CoCr alloys of fixed and removable dental restorations and appliances are reflected in ISO 2267430.

Few studies have compared the mechanical properties of cast, milled, and AM alloys.[31-33] In 2014, Al Jabbari et al[32] found that manufacturing with casting, milling or SLM techniques influenced the hardness and microstructural characterization of CoCr dental alloys. Statistically significant hardness values were found among the groups; the SLM group (371 ± 10 HV) was measured to be the highest, followed by the cast (320 ± 12 HV) and milled (297 ± 5 HV) groups. The alloy microstructure was also significantly different. Radiographs revealed the presence of porosity only in the cast group. Although there was an effort to employ a single CoCr alloy for all the groups, the manufacturing methods required different CoCr alloys.

In 2013, Takaichi et al[34] demonstrated that SLM CoCr specimens fabricated at different angulations between the building direction and tensile direction (0, 45, and 90 degrees) presented differences in their mechanical properties. Specimens with a zero angle (where the building and tensile directions were parallel) demonstrated the highest tensile strengths and elongation after fracture.

CoCr objects manufactured through SLS or SLM technologies are deformed by thermal stress due to rapid heating and cooling during the fabrication process.[34] Moreover, CoCr alloys present multiple variations in chemical composition and microstructure, and their mechanical properties vary in composition, even in the as-cast condition.[34] This internal thermal residual stress can generate strain, and reduces the accuracy of the framework.[35,36] Recently, a heat treatment after fabrication was employed to decrease the residual internal stress, but some authors concluded that the microstructure may also change as a result.[33,37] Furnace requirements for a heat treatment depend on the component material, working temperatures, and atmosphere in the furnace (each manufacturer has its own recommendations for the post-processing heat treatment).

The reduced porosity in mechanical structures fabricated through AM technologies improves the mechanical properties of AM CoCr alloys.[33] Compared with cast alloys, AM CoCr alloys can be used to fabricate frameworks with a higher yield and higher tensile strength.[38] Additionally, similar to conventional processing, SLM CoCr specimens resist corrosion.[39-41]

The mechanical properties of Ti (Ti_6Al_4V) alloy are provided by the various manufacturers (Table 4). Ti_6Al_4V is regarded as a two-phase material, consisting of a hexagonal close-packed (hcp) α phase and a body-centered cubic (bcc) β phase.[42] The transition temperature between the two phases for Ti_6Al_4V is 995°C.[43,44] The mechanical properties of the two-phase Ti_6Al_4V alloy depend on the microstructure and distribution of the two phases throughout the material.[43,45]

SLM technology is used more commonly than EBM technologies in the manufacturing of FDPs. Previous studies have reported that, when manufacturing Ti_6Al_4V products, SLM technology produces more rapid cooling than EBM fabrication, resulting in transformation to α' martensite in various

Table 2 Physical and mechanical properties of CoCr-manufactured alloys (after stress relief) provided by their manufacturers

Property	EOS MP1	EOS SP2	Renishaw	Concept Laser	3D Systems ASTM F75	3D Systems 3DS Dentwise	BEGO
Alloy type ISO 22674	4	4	4	5	5	4	5
Density (g/cm^3)	8.3	8.5	8.5	8.6	8.35	8.8	8.5
Tensile strength (MPa)	1100	1350	1097–1104	1030	1000	910	1150–1400
Yield strength (MPa)	600	850	683–714	635	650	650	790–1000
Elongation at break (%)	20	3	16–21	10	20	8	9
Young's modulus (GPa)	200	200	220	230	230	200	210
Hardness (HV)	350–450	420	400–412	Not available	400	310	360
Coefficient thermal expansion	13.6 x 10-6/ºC	14.5 x 10-6/ºC	10.2 x 10-6/ºC	10.1 x 10-6/ºC	14.3 x 10-6/ºC	14.0 x 10-6/ºC	14.1 x 10-6/ºC
Melting interval (ºC)	1350–1430	1410–1450	1260–1482	1320–1420	1350–1430	1305–1400	1370–1420

Table 3 Chemical composition of Ti powder alloys provided by their manufacturers

Brand name	Composition (% wt)	
EOS DMLS Ti64ELI	Ti: Balance Al: 5.5–6.5 V: 3.5–4.5 O < 0.110	N < 0.04 C < 0.08 H < 0.012 Fe < 0.250 Y < 0.005
Renishaw Ti6Al4V ELI-0406	Ti: Balance Al: 5.5–6.75 V: 3.5–4.5 O < 0.2	N < 0.05 C < 0.08 H < 0.015 Fe < 0.3
Concept Laser	Not available	
3D Systems LaserForm Ti Grade 23	Ti: Balance Al: 5.5-6.5 V: 3.5-4.5 O < 0.13	N < 0.03 C < 0.08 H < 0.012 Fe < 0.25 Y < 0.005
Arcam EBM Ti6Al4V ELI	Ti: Balance Al: 5.5–6-5 V: 3.4–4.5 O < 0.13	N < 0.05 C < 0.08 H < 0.012 Fe < 0.25

Table 4 Physical and mechanical properties of Ti-manufactured alloys provided by their manufacturers

Property	EOS Ti64ELI	Renishaw	Concept Laser	3D Systems	Arcam EBM
Grade	Not available	Not available	Not available	23	5
Density (g/cm^3)	4.41			4.42	Not available
Tensile strength (MPa)	1070			940	860
Yield strength (MPa)	1010			850	795
Elongation at break (%)	14			15	10
Young's modulus (GPa)	Not available			105–120	114
Hardness (HV)	34			30	Not available
Coefficient thermal expansion	Not available			9.7 x 10-6/ºC	Not available
Melting interval (ºC)	Not available			1692–1698	Not available

proportions. This microstructure refinement appears to have a significant effect on the corrosion potential, which may be especially significant for dental applications.[42] However, if sufficient care is taken to utilize only low-oxygen content powder for EBM fabrication, the microstructures can be manipulated to exhibit improved mechanical properties.[29]

Different studies compared the mechanical properties of Ti_6Al_4V alloys manufactured with either AM or conventional casting procedures. In 2009, Murr et al[46] compared the microstructures and mechanical properties of Ti_6Al_4V alloy fabricated by EBM with cast alloy. Compared with the very best-wrought Ti_6Al_4V alloy, the authors concluded that EBM could deliver comparable strength and elongation. The average microindentation hardness of the EBM-manufactured product ranged from 3.6 to 3.9 GPa, and the Vickers microindentation hardness was measured to be 4.0 GPa. Values of ultimate tensile strength (UTS) for EBM samples averaged 1.18 GPa, with elongations ranging from 16% to 25%. Compared with traditional casting methods, AM technologies afford higher definitive product density, reduce manufacturing time and costs, minimize human errors, and prevent casting defects.

Dental applications

Removable partial dentures (RPDs)

By combining the use of intraoral scanners (IOSs) and new manufacturing processes, a completely digital workflow is now possible.[47-53] However, characteristics of the edentulous spaces such as mobile tissue, lack of obvious anatomic landmarks or difficulties in maintaining a dry field can influence the accuracy of a digital impression.[54-56] Therefore, in many cases it may be more practical to combine both digital and conventional procedures to manufacture RPDs.[47-53]

In 2004, Williams et al[47] described a technique for digitally surveying a definitive cast, a CAD design, and a stereolithographic AM resin pattern fabrication to cast a metal framework for a RPD prostheses. In 2006, Williams et al[48,49] developed a technique for the SLM AM CoCr technology for manufacturing RPD frameworks.

Kattadiyil et al[50] closed the digital workflow by incorporating intraoral digital impressions (Cadent iTero, San Jose, CA, USA) of a partially edentulous maxillary arch (Kennedy Class III) for the fabrication of an RPD. The case report describes a digital impression in which 28 scans of the maxillary teeth (both with and without occlusion), 25 scans to enhance the capture of the rest seats, and 28 scans for the mandibular teeth were needed in a total of 17 min. However, digital impressions are limited by the ability of the IOS to capture appropriate extensions of movable body tissue, which would be otherwise captured through conventional methods by border molding the impression material. The digital design of the RPD was completed and the castable framework pattern manufactured using a 3D printer, but the selected AM technology, the 3D printer used, and the castable printed material were not specified in the report.

In 2014, Kanazawa et al[51] reported a protocol for creating a Ti_6Al_4V alloy framework with a layer thickness of 30 µm for a complete maxillary denture using SLM technology. The digitalization of the definitive plaster cast was executed with a 3D cone beam computed tomography (CBCT) system, and the digital design was completed using nondental CAD software (Freeform; Geomatic).

In 2017, Lee et al[57] measured the internal fit of 10 RPDs made on 10 patients using the silicone replica technique. The authors combined the conventional procedures and included the digitalization of the master cast with surveying and RPD framework design. The framework was printed using castable material and a multijet 3D printer. No differences were found among participants with different Kennedy classifications, but significant differences were found in the internal discrepancy of various framework components. The discrepancy under the periphery of the rest was determined to be smaller than that of the center, especially for the cingulum rest. However, no group control was determined, as no comparisons were made with RPDs fabricated using conventional procedures.

Overdentures

In 2015, Lin et at[52] reported a technique for the SLM CoCr superstructure framework of an implant-supported, removable complete overdenture using a combination of both digital and conventional methods. The process began using an IOS to register implant positions and soft tissue morphology. Then, an SM process produced a milled bar with an infrastructure framework, and an AM process fabricated a friction fit using a superstructure framework.

Tooth-supported crowns and fixed dental prostheses (FDPs)

AM technologies to fabricate metal frameworks were also introduced for tooth-supported crowns and FDPs; however, the only metal available in dentistry today is CoCr alloy (Fig 4a). Gold alloys can be processed using AM technologies, but the cost is very high, and they are not used in dentistry.

Different studies have analyzed the marginal and internal discrepancy of AM metal frameworks[55-57] as well as the ceramic bond strength of 3D-printed metals.[65-70] Most studies report a clinically acceptable marginal and internal fit as well as a metal-ceramic bond strength comparable to conventional casting methods.

Marginal and internal discrepancy

One key criterion for the clinical success of restorations is an acceptable marginal and internal discrepancy.[55-57] Published studies have reported that the marginal discrepancy of SLM CoCr metal crowns was within the clinically accepted range, and some authors have described a better fit than that of cast CoCr metal crowns.[63-69]

Örtorp et al[66] evaluated the marginal and internal discrepancy of 32 three-unit CoCr FDPs manufactured using various fabrication methods: the conventional handmade lost wax technique, milled wax pattern and cast, milled, and direct metal laser sintering (DMLS). All measurements were made on longitudinal cuts of the cemented (dual-cure resin cement with a pressure of 50 N) frameworks on master acrylic resin casts with a stereomicroscope. The best fit was found in the DMLS group (84 ± 6 µm), followed by the cast groups (milled 117 ± 9 µm and handmade 133 ± 9 µm wax pattern) and milled group (166 ± 2 µm). However, only vertical discrepancies were examined, and no horizontal planes were measured.

Kim et al[67] compared the marginal discrepancy of a CoCr metal framework of a tooth-borne crown among pre-sintered milled, cast, and SLS-manufactured groups. The 3D gap was calculated by superimposing the CAD reference cast (digitalized study cast) and a 3D replica (digitalized silicone replica) with specified software. The pre-sintered milled group presented the smallest gap (32 ± 5 µm), followed by the SLS-manufactured group (47.3 ± 9 µm), and then the lost wax and casting group (64.1 ± 14 µm). However, the absolute marginal discrepancy cannot be measured with this measuring technique because the digital replica is not able to accurately obtain data from the line of the margin.

Tamac et al[68] analyzed the marginal and internal discrepancy of 60 CoCr metal molar crowns from 42 patients. The crowns were fabricated using three different methods: casting, milling, and DMLS. Silicone replicas were obtained from all the crowns before the luting procedures in order to evaluate the fit with a stereomicroscope. No statistically significant differences were found among the three groups at the marginal fit and axial wall region, but the internal gap at the occlusal and axio-occlusal regions, respectively, were higher for the DMLS group (290.1 ± 112 µm and 188.1 ± 69 µm) than for the milled (265.7 ± 90 µm and 141.1 ± 53 µm) and the cast (201.1 ± 67 µm and 140.6 ± 48 µm) groups.

Huang et al[69] evaluated 330 single-unit CoCr metal ceramic crowns from 274 patients. Each crown was randomly assigned to one of three groups: SLM CoCr, cast CoCr, and cast Au-Pt. An impression replica technique was used to replicate and measure the marginal and internal discrepancy of the crowns using a stereomicroscope. The SLM CoCr crowns demonstrated a similar marginal discrepancy (75.6 ± 32.6 µm) to that of the cast Au-Pt crowns (76.8 ± 32.1 µm) and a better marginal discrepancy than that of the cast CoCr crowns (91 ± 36.3 µm). For the internal gap, only at the occlusal region, the SLM CoCr group (309.8 ± 106.6 µm) was less accurate than the cast CoCr (254.6 ± 109.6 µm) and the cast Au-Pt (249.6 ± 110.4 µm) groups.

Ceramic bond strength

The ceramic bond strength of AM CoCr metal alloys has also been reported to be superior to the current standards of ceramic bond strength, surpassing the minimum acceptable strength of 25 MPa required by AINSA/ADA specification No. 38 (2000) and ISO 9693:1999(E) using the three-bending test.[68-73]

In 2008, Akova et al[70] compared the shear bond strength of SLS CoCr, cast CoCr, and cast NiCr alloys. There were no statistically significant differences in bond strength among the groups. The results also indicated that the cast groups exhibited a mixed mode of cohesive and adhesive failure, whereas half of the samples from the SLS CoCr group presented adhesive failure.

Xiang et al[71] also evaluated this property between SLM CoCr and cast CoCr specimens using the three-bending test. All the samples met the minimum acceptable strength of 25 MPa; furthermore, the SLM CoCr samples exceeded this value (44 MPa). These results coincide with the 2014 study by Wu et al[72] that reported a bond strength of 57 MPa for SLM CoCr alloy.

In 2016, Wang et al[73] evaluated the metal-ceramic bond characteristics of CoCr alloys prepared using three manufacturing processes: casting, milling, and SLM. The oxidation surface before the porcelain application and the morphology and elemental composition of the metal–ceramic interface were evaluated using a scanning electron microscope (SEM), and the ceramic bond strength was measured using the three-bending test. The authors concluded that the oxidation

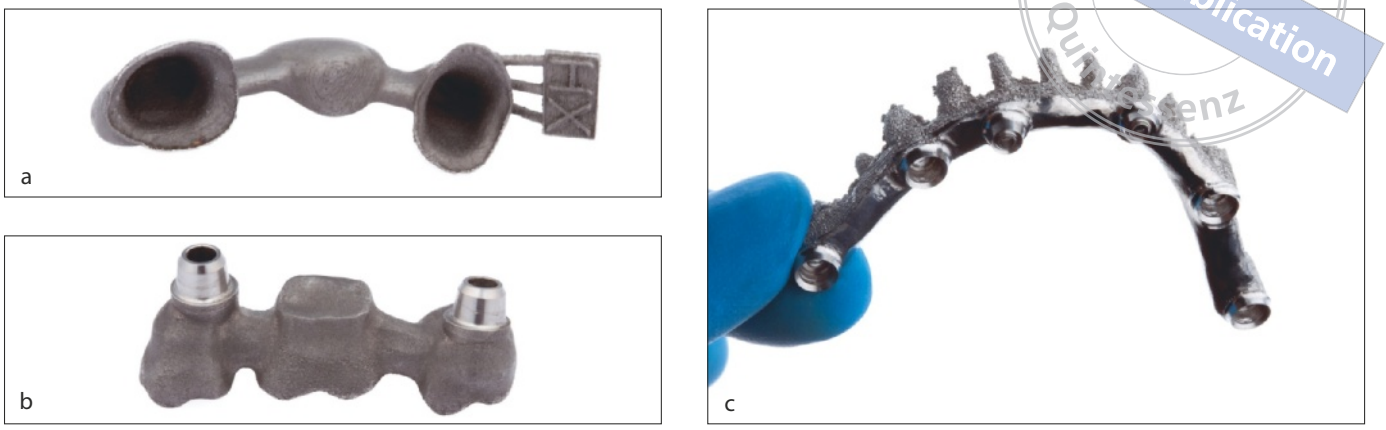

Fig 4 Metal 3D printing applications in dentistry. (a) Tooth-borne 3D-printed CoCr metal framework for a metal-ceramic FDP. (b) Implant-borne SLM AM CoCr metal framework for a metal-ceramic FDP. (c) Complete-arch implant-supported Ti EBM AM framework for a metal-resin FDP.

surface morphologies and thicknesses of dental CoCr alloys depended on the different fabrication techniques used. All the samples had the minimum acceptable strength of 25 Mpa, but the SLM samples exceeded this value (48.6 MPa). No direct relationship was found between failure type and metal–ceramic bond strength.

Ren et al[75] evaluated the effect of multiple firings (three, five, and seven firing cycles) on the ceramic bond strength of SLM and cast CoCr alloys using the three-bending test. These authors measured the silicon (Si) content of specimens with a SEM and energy-dispersive x-ray spectroscopy (EDS). The bond strength was greater than 25 MPa at all firing periods for all the samples, but the SLM group performed better in area fraction of adherence porcelain (AFAP) than the conventionally cast group, especially after five or seven firings.

Zeng et al[76] evaluated the effect of multiple firing (three, five, and seven firing cycles) on the marginal fit of a SLM CoCr and cast metal-ceramic crown using the silicone replica technique and a stereomicroscope. The marginal fit of the SLM group was significantly better than that of the cast group at all firing periods. The mean marginal gap width values for the SLM CoCr group were 36, 37, 38, and 38 mm for the one, three, five, and seven firing cycles, respectively, while the mean marginal gap width values for the cast group were 67, 71, 72, and 73 mm for the same firing periods, respectively.

Implant-supported fixed dental prostheses (FDPs)

AM technologies can be used to manufacture implant-supported FDPs. However, because of the rough surface texture of AM metal frameworks, milling the implant interface is a practical measure (Fig 4b and c). Manufacturing companies have developed a combination of additive and subtractive procedures to fabricate implant-supported FDPs. The first step is printing the metal framework, contouring over the implant interface (Fig 5a and b). The second step is milling the desired connection on the implant interface (Fig 5c and d).

Revilla-León et al[77] documented the fabrication of a maxillary and mandibular implant-supported FDP for a completely edentulous patient. Metal frameworks were manufactured using AM procedures. A metal-ceramic FDP was created for the maxillary arch using SLM CoCr technology; on the mandibular arch, a metal-acrylic resin FDP was manufactured using EBM technology.

Revilla-León et al[78] analyzed implant-prosthesis discrepancies and distortions on the x-, y-, and z-axis of Ti frameworks fabricated with SLM or EBM processes, which were fabricated for implant-supported complete-arch prostheses. Measurements were taken using a coordinate measuring machine (CMM). The mean implant–prosthesis 3D discrepancies were 67 ± 13.5 µm and 60.2 ± 18.5 µm for the SLM and EBM technologies, respectively. No significant differences were observed in the x- and y-axis ($P > 0.05$). The mean discrepancy of the z-axis, representing the occlusogingival discrepancy, was 6.2 ± 6.1 µm and 13.6 ± 6.2 µm for the Ti SLM and EBM frameworks, respectively. To evaluate the accuracy of the manufacturing procedures, the STL file and the AM frameworks were compared, revealing a mean discrepancy of 39.2 ± 27.0 µm on the x-axis, 37 ± 14.8 µm on the y-axis, 6.5 ± 1.8 µm on the z-axis, and 60.6 ± 12.6 µm in the 3D discrepancy analysis. Within the limitations of the study, the authors concluded that the Ti frameworks for a com-

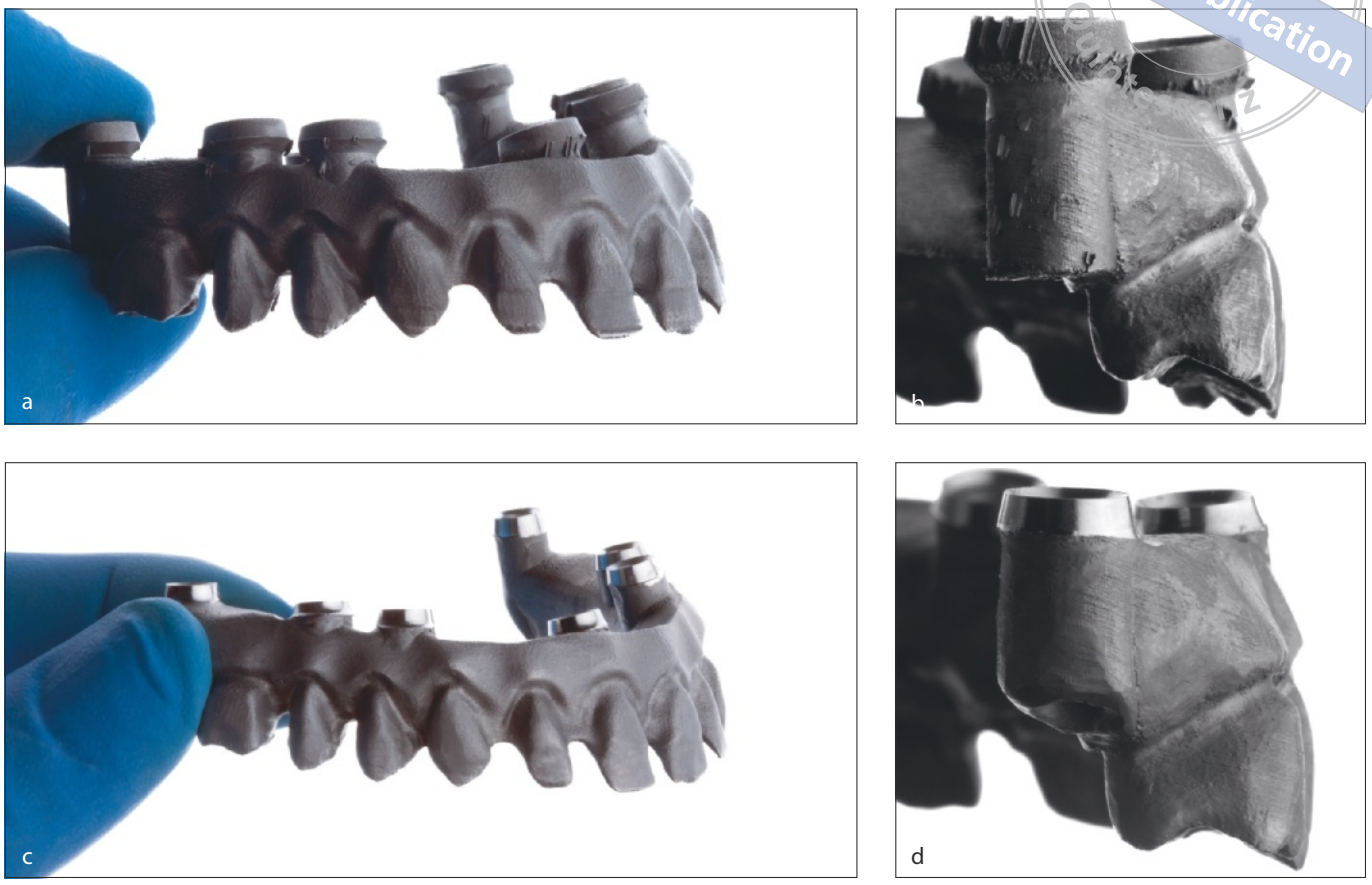

Fig 5 Metal-printed framework procedure for implant-supported FDPs. (a) Metal 3D-printing framework manufactured using a SLM technology before milling the implant interface. (b) Detail of the overcontoured implant interface just printed using a SLM technology. (c) 3D-printed framework with subsequent CNC machining of the implant interface. (d) Detail of the milled implant interface.

plete-arch implant-supported prosthesis fabricated using either SLM or EBM AM technologies demonstrated clinically acceptable implant–prosthesis discrepancies. In addition, the discrepancies were similar across both AM technologies. Both AM technologies showed comparable and adequate capabilities to accurately translate STL file data into frameworks.

Frameworks for the implant impression technique

Revilla-León et al[79] described a technique for the fabrication of a complete-arch implant with a splinting metal framework and a custom polymer tray using AM technologies. The framework was manufactured using SLM technology (Fig 6). However, any metal AM technology would have sufficiently fulfilled the purpose of splinting the impression implant abutments. This technique provides a high degree of control over the thickness of the tray, splinting material, and impres-

Fig 6 3D-printed metal splinting structure for a complete-arch implant impression technique.

sion material during the clinical procedure, reducing both time and costs in the chair and in the laboratory. CAD software (Dental System; 3Shape) was employed to digitally design the framework and custom tray.

In 2018, Piedra Cascón et al[80] described the same procedure, but using highly accessible open source software. Time is an important consideration during the CAD design phase. However, the authors stated that, once the learning curve had been overcome, the 3D design process of the splinting framework and tray should take no more than 10 to 15 min. This proficiency ultimately depends on the expertise of the clinician or dental technician.

Summary

AM technologies are reliable for many applications in dentistry, including metal frameworks for RPDs, overdentures, tooth- and implant-supported FDPs, and metal frameworks for splinting implant impression abutments. However, further studies are needed in future to evaluate their accuracy, reproducibility, and clinical outcome throughout function. Nevertheless, technological improvements in the future and the incorporation of newly approved materials will allow for broader applications in dentistry.

Disclaimer

The authors have no commercial interest in any of the materials discussed in this study.

References

1. Singh V. Rapid Prototyping, Materials for RP and Applications of RP. IJSER 2013;4:473–480.
2. Van Noort R. The future of dental devices is digital. Dent Mater 2012:28:3–12.
3. Horn TJ, Harrysson OL. Overview of current additive manufacturing technologies and selected applications. Sci Prog 2012:95:255–282.
4. Tapie L, Lebon N, Mawussi B, Fron-Chabouis H, Duret F, Attal JP. Understanding dental CAD/CAM for restorations – accuracy from a mechanical engineering viewpoint. Int J Comput Dent 2015;18: 343–367.
5. Strub JR, Rekow ED, Witkowski S. Computer-aided design and fabrication of dental restorations: current systems and future possibilities. J Am Dent Assoc 2006;137:1289–1296.
6. Beuer F, Schweiger J, Edelhoff D. Digital dentistry: an overview of recent developments for CAD/CAM generated restorations. Br Dent J 2008;204:505–511.
7. Lebon N, Tapie L, Duret F, Attal JP. Understanding dental CAD/CAM for restorations – dental milling machines from a mechanical engineering viewpoint. Part A: chairside milling machines. Int J Comput Dent 2016;19:45–62.
8. Torabi K, Farjood E, Hamedani S. Rapid Prototyping Technologies and their Applications in Prosthodontics, a Review of Literature. J Dent (Shiraz) 2015;16:1–9.
9. Witkowski S. CAD/CAM in Dental Technology. Quintessence Dent Technol 2005;28:169–184.
10. ASTM, Committee F42 on Additive Manufacturing Technologies, West Conshohocken, Pa. 2009 Standard terminology for additive manufacturing – general principles and terminology. ISO/ ASTM52900–15.
11. StereoLithography Interface Specification, 3D Systems, Inc., 1988. Valencia, CA.
12. Deckard C, Beaman J. Process and control issues in selective laser sintering. ASME Prod Eng Div 1988;33:191–197.
13. Deckard CR. 1986. Patent US 4863538-A. Method and apparatus for producing parts by selective sintering.
14. Mazzolini A. Selective laser sintering in biomedical engineering. Med Biol Eng Comput 2013;51:245–256.
15. Fisher P, Karapatis N, Romano V, Weber HP. A model for the interaction of near infrared pulsed laser with metal powders in selective laser sintering. Appl Phys A 2002;74:467–474.
16. Anestiev LA, Froyen L. Model of primary rearrangement processes at liquid phase sintering and selective laser sintering due to biparticle interactions. J Appl Phys 1999;86:4008.
17. Traini T, Mangano C, Sammons RL, Mangano F, Macchi A, Piattelli A. Direct laser metal sintering as a new approach to fabrication of an isoelastic functionally graded material for manufacture of porous titanium dental implants. Dent Mater 2008;24:1525–1533.
18. Horn TJ, Harrysson OL. Overview of current additive manufacturing technologies and selected applications. Sci Prog 2012;95:255–282.
19. Vandenbroucke B, Kruth JP. Selective laser melting of biocompatible metals for rapid manufacturing of medical parts. Rapid Prototyping J 2007;13:196–203.
20. Osakada K, Shiomi M. Flexible manufacturing of metallic products by selective laser melting of powder. Int J Machine Tools Manuf 2006;46:1188–1193.
21. Murr LE, Gaytan SM, Ramirez DA, et al. Metal fabrication by additive manufacturing using laser and electron beam melting technologies. J Mater Sci Technol 2012;28:1–14.
22. Koutsoukis T, Zinelis S, Eliades G, Al-Whazzan K, Rifaiy MA, Al Jabbari YS. Selective laser melting technique of Co-Cr dental alloys: a review of structure and properties and comparative analysis with other available techniques. J Prosthodont 2015;24:303–312.
23. Alcisto J, Enriquez A, Garcia H, et al. Tensile Properties and Microstructures of Laser-Formed Ti-6Al-4V. JMEPEG 2011;20:203–212.
24. Abd-Elghany K, Bourrell DL. Property evaluation of 304L stainless steel fabricated by selective laser melting. Rapid Prototyping J 2012;18:420–428.
25. Vijay Venkatesh K, Vidyashree Nandini V. Direct Metal Laser Sintering: A Digitised Metal Casting Technology. J Indian Prosthodont Soc 2013;13:389–392.

26. AMS 4999 Specification, 2002. Titanium Alloy Laser Deposited Products 6Al-4V Annealed, SAE, Warrendale, PA.
27. Niinomi M. Mechanical biocompatibilities of titanium alloys for biomedical applications. J Mech Behav Biomed Mater 2008;1:30–42.
28. Hollander DA, Von Walter M, Wirtz T, et al. Structural, mechanical and in vitro characterization of individually structured Ti-6Al-4V produced by direct laser forming. Biomater 2006;27:955–963.
29. Koike M, Greer P, Owen K, et al. Evaluation of Titanium Alloys Fabricated Using Rapid Prototyping Technologies – Electron Beam Melting and Laser Beam Melting. Materials (Basel) 2011;4:1776–1792.
30. International standard ISO 22674. Dentistry – Metallic materials for fixed and removable restorations and appliances, ed 2, 2016.
31. Qian B, Saeidi K, Kvetková L, Lofaj F, Xiao C, Shen Z. Defects-tolerant Co-Cr-Mo dental alloys prepared by selective laser melting. Dent Mater 2015;31:1435–1444.
32. Al Jabbari YS, Koutsoukis T, Barmpagadaki X, Zinelis S. Metallurgical and interfacial characterization of PFM Co-Cr dental alloys fabricated via casting, milling or selective laser melting. Dent Mater 2014;30:e79–e88.
33. Koutsoukis T, Zinelis S, Eliades G, Al-Wazzan K, Rifaiy MA, Al Jabbari YS. Selective Laser Melting Technique of Co-Cr Dental Alloys: A Review of Structure and Properties and Comparative Analysis with Other Available Techniques. J Prosthodont 2015;24:303–312.
34. Takaichi A, Suyalatu, Nakamoto T, et al. T. Microstructures and mechanical properties of Co-29Cr-6Mo alloy fabricated by selective laser melting process for dental applications. J Mech Behav Biomed Mater 2013;21:67–76.
35. Kruth JP, Froyen L, Van Vaerenbergh J, Mercelis P, Rombouts M, Lauwers B. Selective laser melting of iron-based powder. J Mater Process Technol 2004;149:616–622.
36. Shiomi M, Osakada K, Nakamura K, Yamashita T, Abe F. Residual stress within metallic model made by selective laser melting process. CIRP Annals 2004;53:195–198.
37. Mantrala KM, Das M, Balla VK, Rao CS, Kesava Rao VVS. Additive manufacturing of Co-Cr-Mo alloy: influence of heat treatment on microstructure, tribiological, and electrochemical properties. Front Mech Eng 2015;1:2.
38. Jevremovic D, Puskar T, Kosec B, et al. The analysis of the mechanical properties of F75 Co–Cr alloy for use in selective laser melting (SLM) manufacturing of removable partial dentures (RPD). Metalurgija 2012;51:171–174.
39. Zeng L, Xiang N, Wei B. A comparison of corrosion resistance of cobalt- chromium-molybdenum metal ceramic alloy fabricated with selective laser melting and traditional processing. J Prosthet Dent 2014;112:1217–1224.
40. Serra-Prat J, Cano-Batalla J, Cabratosa-Termes J, Figueras-Àlvarez O. Adhesion of dental porcelain to cast, milled, and laser-sintered cobalt-chromium alloys: shear bond strength and sensitivity to thermocycling. J Prosthet Dent 2014;112:600–605.
41. Lu Y, Wu S, Gan Y, et al. Investigation on the microstructure, mechanical property and corrosion behavior of the selective laser melted CoCrW alloy for dental application. Mater Sci Eng C Mater Biol Appl 2015;49:517–525.
42. Donachie MJ. Titanium: A Technical Guide, ed 2. Materials Park, OH: ASM International, 2000:95–123.
43. Ding R, Guo Z, Wilson A. Microstructural evolution of a Ti-6Al-4V alloy during thermomechanical processing. Mater Sci Eng A 2002;327:233–245.
44. Lütjering G, Williams JC. Titanium, ed 2. Berlin: Springer, 2007:86–103.
45. Lütjering G. Influence of processing on microstructure and mechanical properties of (α+β) titanium alloys. Mater Sci Eng A 1998;243:32–45.
46. Murr LE, Esquivel EV, Quinones SA, et al. Microstructures and mechanical properties of electron beam-rapid manufactured Ti-6Al-4V biomedical prototypes compared to wrought Ti-6Al-4V. Mater Char 2009;60:96–105.
47. Williams RJ, Bibb R, Rafik T. A technique for fabricating patterns for removable partial denture frameworks using digitized casts and electronic surveying. J Prosthet Dent 2004;91:85–88.
48. Williams RJ, Bibb R, Eggbeer D, Collis J. Use of CAD/CAM technology to fabricate a removable partial denture framework. J Prosthet Dent 2006;96:96–99.
49. Williams RJ, Eggbeer D, Bibb R. CAD/CAM rapid manufacturing techniques in the fabrication of removable partial denture frameworks. Quintessence J Dent Technol 2008;6:42–50.
50. Kattadiyil MT, Mursic Z, AlRumaih H, Goodacre CJ. Intraoral scanning of hard and soft tissues for partial removable dental prosthesis fabrication. J Prosthet Dent 2014;112:444–448.
51. Kanazawa M, Iwaki M, Minakuchi S, Nomura N. Fabrication of titanium alloy frameworks for complete dentures by selective laser melting. J Prosthet Dent 2014;112:1441–1447.
52. Lin WS, Chou JC, Metz MJ, Harris BT, Morton D. Use of intraoral digital scanning for a CAD/CAM-fabricated milled bar and superstructure framework for an implant-supported, removable complete dental prosthesis. J Prosthet Dent 2015;113:509–515.
53. Alifui-Segbaya F, Williams RJ, George R. Additive Manufacturing: A Novel Method for Fabricating Cobalt-Chromium Removable Partial Denture Frameworks. Eur J Prosthodont Restor Dent 2017;25:73–78.
54. Andriessen FS, Rijkens DR, van der Meer WJ, Wismeijer DW. Applicability and accuracy of an intraoral scanner for scanning multiple implants in edentulous mandibles: a pilot study. J Prosthet Dent 2014;111:186–194.
55. Patzelt SB, Vonau S, Stampf S, Att W. Assessing the feasibility and accuracy of digitizing edentulous jaws. J Am Dent Assoc 2013;144:914–920.
56. Flügge TV, Att W, Metzger MC, Nelson K. Precision of Dental Implant Digitization Using Intraoral Scanners. Int J Prosthodont 2016;29:277–283.
57. Lee JW, Park JM, Park EJ, Heo SJ, Koak JY, Kim SK. Accuracy of a digital removable partial denture fabricated by casting a rapid prototyped pattern: A clinical study. J Prosthet Dent 2017;118:468–474.
58. Coli P, Karlsson S. Fit of a new pressure-sintered zirconium dioxide coping. Int J Prosthodont 2004;17:59–64.
59. Chan C, Haraszthy G, Geis-Gerstorfer J, Weber H, Huettemann H. Scanning electron microscopic studies of the marginal fit of three esthetic crowns. Quintessence Int 1989;20:189–193.
60. Rudd RW, Rudd KD. A review of 243 errors possible during the fabrication of a removable partial denture: part I. J Prosthet Dent 2001;86:251–261.

61. Xu D, Xiang N, Wei B. The marginal fit of selective laser melting-fabricated metal crowns: an in vitro study. J Prosthet Dent 2014;112:1437–1440.
62. Huang Z, Zhang L, Zhu J, Zhao Y, Zhang X. Clinical Marginal and Internal Fit of Crowns Fabricated Using Different CAD/CAM Technologies. J Prosthodont 2015;24:291–295.
63. Huang Z, Zhang L, Zhu J, Zhang X. Clinical marginal and internal fit of metal ceramic crowns fabricated with a selective laser melting technology. J Prosthet Dent 2015;113:623–627.
64. Ucar Y, Akova T, Akyil MS, Brantley WA. Internal fit evaluation of crowns prepared using a new dental crown fabrication technique: laser-sintered Co-Cr crowns. J Prosthet Dent 2009;102:253–259.
65. Quante K, Ludwig K, Kern M. Marginal and internal fit of metal-ceramic crowns fabricated with a new laser melting technology. Dent Mater 2008;24:1311–1315.
66. Örtorp A, Jönsson D, Mouhsen A, Vult von Steyern P. The fit of cobalt-chromium three-unit fixed dental prostheses fabricated with four different techniques: a comparative in vitro study. Dent Mater 2011;27:356–363.
67. Kim KB, Kim JH, Kim WC, Kim JH. Three-dimensional evaluation of gaps associated with fixed dental prostheses fabricated with new technologies. J Prosthet Dent 2014;112:1432–1436.
68. Tamac E, Toksavul S, Toman M. Clinical marginal and internal adaptation of CAD/CAM milling, laser sintering, and cast metal ceramic crowns. J Prosthet Dent 2014;112:909–913.
69. Huang Z, Zhang, Zhu J, Zhang X. Clinical marginal and internal fit of metal ceramic crowns fabricated with a selective laser melting technology. J Prosthet Dent 2015;113:623–627.
70. Akova T, Ucar Y, Tukay A, Balkaya MC, Brantley WA. Comparison of the bond strength of laser-sintered and cast base metal dental alloys to porcelain. Dent Mater 2008;24:1400–1404.
71. Xiang N, Xin XZ, Chen J, Wei B. Metal-ceramic bond strength of Co-Cr alloy fabricated by selective laser melting. J Dent 2012;40:453–457.
72. Wu L, Zhu H, Gai X, Wang Y. Evaluation of the mechanical properties and porcelain bond strength of cobalt-chromium dental alloy fabricated by selective laser melting. J Prosthet Dent 2014;111:51–55.
73. Wang H, Feng Q, Li N, Xu S. Evaluation of metal-ceramic bond characteristics of three dental Co-Cr alloys prepared with different fabrication techniques. J Prosthet Dent 2016;116:916–923.
74. Li J, Chen C, Liao J, et al. Bond strengths of porcelain to cobalt-chromium alloys made by casting, milling, and selective laser melting. J Prosthet Dent 2017;118:69–75.
75. Ren XW, Leng L, Wei ZM, Xin XZ, Wei B. Effects of multiple firings on metal-ceramic bond strength of Co-Cr alloy fabricated by selective laser melting. J Prosthet Dent 2016;115:109–114.
76. Zeng L, Zhang Y, Liu Z, Wei B. Effects of repeated firing on the marginal accuracy of Co-Cr copings fabricated by selective laser melting. J Prosthet Dent 2015;113:135–139.
77. Revilla-León M, Klemm IM, García-Arranz J, Özcan M. 3D metal printing – additive manufacturing technologies for frameworks of implant-borne fixed dental prostheses. Eur J Prosthodont Restor Dent 2017;25:143–147.
78. Revilla-León M, Ceballos L, Martínez-Klemm I, Özcan M. Discrepancy of complete-arch titanium frameworks manufactured using selective laser melting and electron beam melting additive manufacturing technologies. J Prosthet Dent 2018;120:942–947.
79. Revilla-León M, Sánchez-Rubio JL, Oteo-Calatayud J, Özcan M. Impression technique for a complete-arch prosthesis with multiple implants using additive manufacturing technologies. J Prosthet Dent 2017;117:714–720.
80. Piedra Cascón W, Revilla-León M. Digital workflow for the design and additively manufacture of a splinted framework and custom tray for the impression of multiple implants: A dental technique. J Prosthet Dent 2018;120:805–811.

Verfahren zur additiven Metallfertigung: Literaturreview zum aktuellen Status und zu den prothetischen Einsatzmöglichkeiten

Schlüsselwörter: *3D-Druck, additive Fertigungsverfahren, Elektronenstrahlschmelzen, Metall, selektives Laserschmelzen, selektives Lasersintern, Prothetik*

Zusammenfassung

Ziel: Überprüft werden sollen additive Zirkon-Fertigungsverfahren und zwar jene mit Pulverbettfusionen (PBF) – selektives Lasersintern (SLS), selektives Laserschmelzen (SLM) und Elektronenstrahlschmelzen (EBM) – und ihre derzeitigen Einsatzgebiete in der dentalen Prothetik.
Materialien und Methoden: Nach Sichtung der Literatur wurden die additiven Fertigungsverfahren und ihre aktuellen Einsatzbereiche in der Prothetik zusammengetragen und beschrieben. Datenquellen waren veröffentlichte Artikel über die additive Fertigung von Zirkon in der Zahnheilkunde in MEDLINE, EMBASE, EBSCO und dem Web of Science. Alle Studien befassten sich mit der Beschreibung, Analyse und Evaluation der prothetischen Einsatzbereiche von Verfahren zur additiven Metallfertigung.
Ergebnisse und Schlussfolgerungen: Additive Fertigungsverfahren erbringen bei vielen Einsatzbereichen zuverlässige Ergebnisse. Dazu gehören Metallgerüste von herausnehmbaren Teilprothesen (RPD), Deckprothesen, zahn- und implantatgelagerte Kronen und Brücken (FDP) sowie Metallgerüste für das Verblocken von Abformabutments auf Implantaten. Allerdings sind weitere Studien erforderlich, um ihre Präzision und Reproduzierbarkeit sowie die klinischen Ergebnisse bei funktioneller Belastung zu ermitteln.

Marta Revilla-León

Marta Revilla-León, DDS, MSD
Assistant Program Director, AEGD Program, College of Dentistry, Texas A&M University, Dallas, Texas, USA; Affiliate Faculty Graduate Prosthodontics, University of Washington, Seattle, WA, USA; Researcher, Revilla Research Center, Madrid, Spain

Matthew J. Meyer
Student, College of Dentistry, Texas A&M University, Dallas, Texas, USA

Mutlu Özcan, DDS, DMD, PhD
Professor and Head, Dental Materials Unit, Center for Dental and Oral Medicine, University of Zürich, Switzerland

Address
Marta Revilla-León, DDS, MSD, College of Dentistry, Texas A&M University, 3302 Gaston Avenue, Room 713, Dallas, Texas 75246, USA
Tel.: +1 214 886 0251; E-mail: revillaleon@tamhsc.edu